Numerical simulations of astrophysical cyclotron-maser emission

D.C. Speirs[1], R. Bingham[1,2], K. Ronald[1], A.D.R. Phelps[1], S.L. McConville[1], K.M. Gillespie[1], R.A. Cairns[3], B.J. Kellett[1], I. Vorgul[3], A.W. Cross[1]

[1] *Department of Physics, SUPA, University of Strathclyde, Glasgow, Scotland, G4 0NG, U.K*

[2] *Department of Physics, SUPA, University of Strathclyde, Glasgow, Scotland, G4 0NG, U.K.*

[3] *School of Mathematics and Statistics, University of St. Andrews, Fife, Scotland, KY16 9SS, U.K.*

The electron cyclotron-maser instability plays a significant role in the generation of highly non-thermal, polarised radio emission from the auroral region of planets and stars having a dipole-like magnetic field [1, 2]. More recently, this radiation model has been extended to a variety of astrophysical environments including Blazar jets, collisionless shocks and brown dwarfs [3–7]. Planetary auroral radio emission has been a topic of interest for many years with several mechanisms having been proposed [8–13]. As the dispersion relation describing the electromagnetic wave growth only depends on the factor by which the magnetic field increases and on the ratio of plasma and cyclotron frequencies, the mechanism can scale effectively over many orders of magnitude both in wavelength and spatial scale. In the Earth's auroral region, observations by the Viking spacecraft [11] and the FAST satellite [12] led to the suggestion that the free energy source for AKR is a population of downward accelerated electrons having a large perpendicular velocity produced by a combination of parallel accelerating electric fields and converging magnetic field lines. The electron distribution takes the form of a horseshoe or crescent shape due to the first adiabatic invariance as the electrons move into the stronger magnetic field. Scaled laboratory experiments also demonstrate the potential for horseshoe distributions to generate narrowband cyclotron-maser emission at GHz frequencies over distances of a few meters [15–18].

Although the generation mechanism is well established, there remain important questions with regard to how the radiation may propagate and ultimately escape. Models and observations [19, 20] assume near field-aligned R-mode polarisation prior to escape, however it is well known that the radiation is generated near perpendicular to the magnetic field in the X-mode. The manner by which the radiation may effectively be redirected along the magnetic field and ultimately escape is a question recently addressed by Mutel [20] and Meniett [21], with a model of upward refraction due to altitude variation in the background plasma density and an initial radiation propagation vector that is mildly against the direction of the electron flux (negative axial wavenumber). Current theoretical models for X-mode generation via the cyclotron-maser

instability do not predict growth with a negative axial wavenumber, however we have developed a new theoretical model that clearly demonstrates an enhanced growth rate for finite negative axial wavenumbers and moderate electron energy spread. This model is verified by the results of full 3D PiC (Particle-in-cell) code simulations, demonstrating for the first time that auroral cyclotron-maser emission is indeed characterised by a finite negative axial wavenumber.

The theoretical model [22] assumes an analytic form for the electron distribution function with different pitch angles, energy spread and density ratios between the hot component making up the horseshoe element and a background Maxwellian component. This is then used in a dispersion relation for the R-X mode which is obtainable from the susceptibility tensor given by Stix [23]. The derived growth rate is approximately given by $Im(\omega) = \frac{Im(D)}{\frac{\partial}{\partial\omega}(Re(D))}$, where $D = 0$ is the dispersion relation. The imaginary part $Im(D)$ does not vary greatly for small $\pm n_{\|}$ (where $n_{\|} = k_{\|}c/\omega$) however the value of $\partial D/\partial\omega$ rises dramatically as a function of frequency, due to approaching the upper hybrid resonance, where D has a singularity. This means that the growth rate for positive $n_{\|}$ (higher frequency and forward-wave) is reduced and maximum growth occurs at lower frequency (negative $n_{\|}$ and backward-wave). Beam spreading in velocity space tends to reduce growth rate for negative $n_{\|}$, therefore enhanced backward wave coupling should break down for increased energy or velocity spread.

We compare the theoretical analysis with the results of PiC simulations, undertaken using the particle-in-cell code VORPAL [24]. The simulation geometry comprised an axial length of $144\lambda_{ce}$ (where λ_{ce} is the vacuum wavelength of radiation at the peak electron cyclotron frequency within the simulation) and transverse perfectly-matched-layer boundaries to mitigate reflection. A 20keV electron beam was injected parallel to an axial magnetic field increasing by a factor of 15 over $45\lambda_{ce}$. The peak magnetic flux density was plateaued over the remaining $99\lambda_{ce}$ of beam propagation path to maintain cyclotron resonance for a significant number of Larmor steps with $\omega_{ce}/\omega_{pe} = 20$.

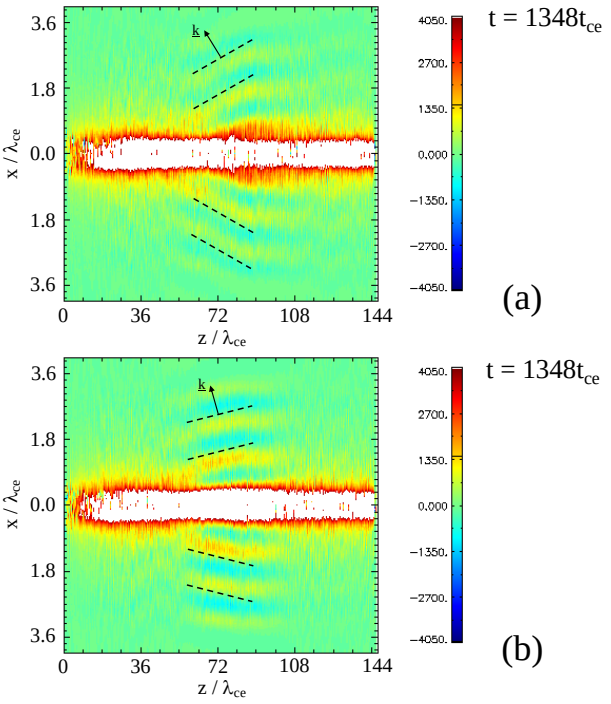

Figure 1: *Contour plots of Ey in an x-z plane at* $t/t_{ce} = 1348$ *for (a) 2% and (b) 6% Gaussian energy spreads*

An analysis of the transverse electric field profile E_y in an x-z plane (Fig. 1b,c) for 2% and 6% energy spread reveals a well-defined and temporally modulated electromagnetic emission at an axial coordinate of $80\lambda_{ce}$ and polarised in the X-mode with a significant negative axial wavenumber (backward-wave component). The backward wave character of emission is evidenced by an oblique wave front propagation angle with respect to the axis of the system. The effective backward-wave angle for 2% energy spread is $\sim 3^\circ$ from perpendicular - consistent with requirements for the aforementioned model of upward refraction of the generated radiation [21]. It is evident in figure 1 that as the energy spread increases to 6%, there is well-defined change in the wavevector with a reduction in backward propagation angle to $\sim 2^\circ$. This emission profile not only indicates a reduction in backward wave coupling with increased energy spread, but a distinct curvature can also be observed in the wavefront for 6% energy spread (figure 1c). This curvature indicates a progressive shift towards perpendicular propagation with increasing axial coordinate, showing that velocity spreading due to cyclotron-wave coupling reduces efficiency for -ve $k_{\|}$. This result is consistent with predictions of the analytical theory.

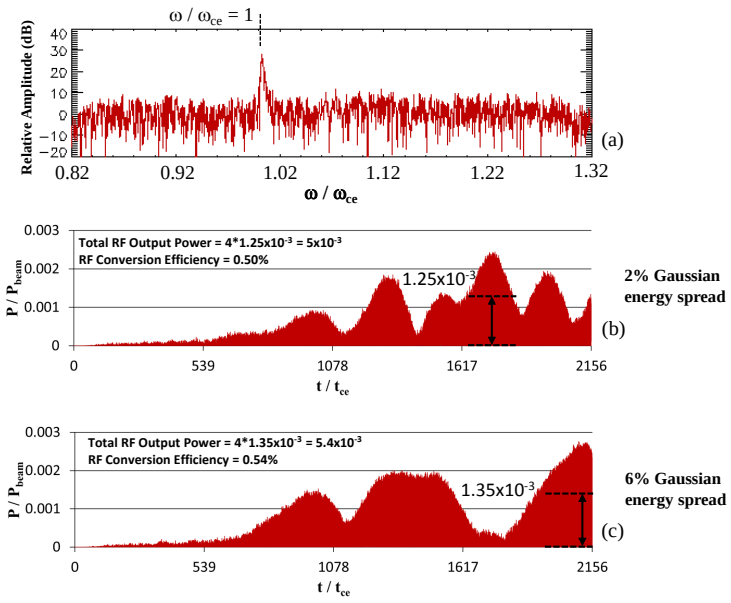

Figure 2: *Contour plots of Ey in an x-z plane at* $t/t_{ce} = 1348$ *for (a) 2% and (b) 6% Gaussian energy spreads*

Figure 2a contains a Fourier transform of E_y at time $2156t_{ce}$ and an axial position of $86\lambda_{ce}$. A single spectral component is present at $\omega/\omega_{ce} = 1$, corresponding to narrowband emission at the relativistic electron cyclotron frequency. Looking at the corresponding transverse Poynting flux over a y-z plane in figure 2b, a temporal modulation to the emission is evident, with a $810t_{ce}$ lead time for significant growth of the radio frequency (RF) Poynting flux. A peak saturated output power of $P/P_{beam} = 1.25 \times 10^{-3}$ is apparent (as the space-time average is $1/2$ of the plotted peak amplitude), which integrated over the transverse dimensions of the system (factoring in the 4 enclosing Poynting flux planes) equates to an RF conversion efficiency of 0.50%. Looking at 6% energy spread (figure 2c) a more stable output is observed, with longer period temporal fluctuations and a marginally increased peak beam-wave conversion efficiency of 0.54%. It would therefore appear that as the electron energy spread is increased, not only

does the wavevector of emission tend from backward-wave to near perpendicular, but a more temporaly stable cyclotron-maser emission process is observed.

In conclusion, we have shown that the electron cyclotron-maser instability driven by a horseshoe-shaped velocity distribution has an inherently enhanced growth rate for wave propagation with finite negative $k_{\|}$ corresponding to a backward-wave propagation angle a few degrees from perpendicular. This natural backward-wave character to the emission serves as a suitable precursor to the recently proposed model of upward refraction and field-aligned escape of terrestrial auroral kilometric radiation [20, 21].

This work was supported by EPSRC grant no. EP/G04239X/1.

References

[1] P. Zarka, Adv. Space Res. **12**, 99 (1992).

[2] R. Bingham, R. A. Cairns, and B. J. Kellett, Astron. Astrophys. **370**, 1000 (2001).

[3] M. C. Begelman, R. E. Ergun, and M. J. Rees, Astrophys. J. **625**, 51 (2005).

[4] R. Bingham, et al., Space Sci. Rev. *10.1007/s11214-013-9963-z* (2013).

[5] R. A. Treumann, Astron. Astrophys. Rev. **13**, 229 (2006).

[6] R. Bingham et al., Astrophys. J. **595**, 279 (2003).

[7] G. Hallinan et al., Astrophys. J. **684**, 644 (2008).

[8] C. S. Wu and L. C. Lee, Astrophys. J. **230**, 621 (1979).

[9] R. M. Winglee and P. L. Pritchett, J. Geophys. Res. **91**, 13531 (1986).

[10] D. B. Melrose, *Instabilities in Space and Laboratory Plasmas* (Cambridge University Press, 1986).

[11] P. Louarn et al., J. Geophys. Res. **95**, 5983 (1990).

[12] R. E. Ergun et al., Astrophys. J. **538**, 456 (2000).

[13] R. Bingham and R. A. Cairns, Phys. Plasmas **7**, 3089 (2000).

[14] A. Roux et al., J. Geophys. Res. **98**, 11657 (1993).

[15] K. Ronald et al., Phys. Plasmas **15**, 056503 (2008).

[16] S. L. McConville et al., Plasma Phys. Controlled Fusion **50**, 074010 (2008).

[17] D. C. Speirs et al., Plasma Phys. Controlled Fusion **50**, 074011 (2008).

[18] A. G. Shalashov et al, Plasma Phys. Controlled Fusion **54**, 085023 (2012).

[19] R. A. Cairns, I. Vorgul, and R. Bingham, Phys. Rev. Lett. **101**, 215003 (2008).

[20] R. L. Mutel, I. W. Christopher, and J. S. Pickett, Geophys. Res. Letters **35**, L07104 (2008).

[21] J. D. Menietti et al., J. Geophys. Res. **116**, A12219 (2011).

[22] D.C. Speirs et al., Physical Review Letters, 113, 155002, (2014).

[23] T. H. Stix, *Waves in Plasma* (AIP, New York, 1992).

[24] C. Nieter and J. R. Cary, J. Comput. Phys. **196**, 448 (2004).